

II-3 THE PRECIPITATION AND WATER VAPOR TRANSPORT OVER AND AROUND THE ARID AND SEMI-ARID REGIONS OF CHINA

YATAGAI Akiyo and YASUNARI Tetsuzo

Institute of Geoscience, University of Tsukuba, Tsukuba, Japan

Abstract

In this study, the rainfall distribution and water vapor transport in and around arid region over Northwest China in summer season have been investigated. The time and space structure of interannual summer precipitation variation of this region is divided to 6 regions by applying rotated EOF analysis. Around Northwest China, there are three regions; 1) North of Tianshan Mountain, 2) south part of Taklimakan desert and 3) the middle reaches of Yellow River, while time series of Zhangye (HEIFE observing station) is classified to 2) south part of Taklimakan desert area.

The water vapor to Taklimakan desert comes from west in the summer mean state. However, in the north of Qilian Shan mountain (and around HEIFE station) the flow from south brings precipitation in most cases.

1. Introduction

In order to understand the mechanism of desertification, the studies of natural variability of precipitation on seasonal, inter-seasonal and interannual scales are important. To understand the basic processes associated with those variation in precipitation, the analysis of weather systems and water vapor transport are also very important.

In the present study, we investigate the time and space structure of precipitation fluctuation in the arid and semiarid region of China, and Mongolia. We also investigate the water vapor transport and precipitation during the warm period in the arid and semi-arid regions of North and Northeast China and its periphery.

In the following sections, the spatial and temporal precipitation characteristics, the mean summer water vapor transport are discussed. We also show some case study of year-to-year variation of water vapor transport associated with the precipitation.

2. Data

The data used in this study were derived from three sources; 1) monthly precipitation data of China (40 stations which annual precipitation are less than 500mm) and Mongolia (23 stations) covering from 1951 to 1990, 2)

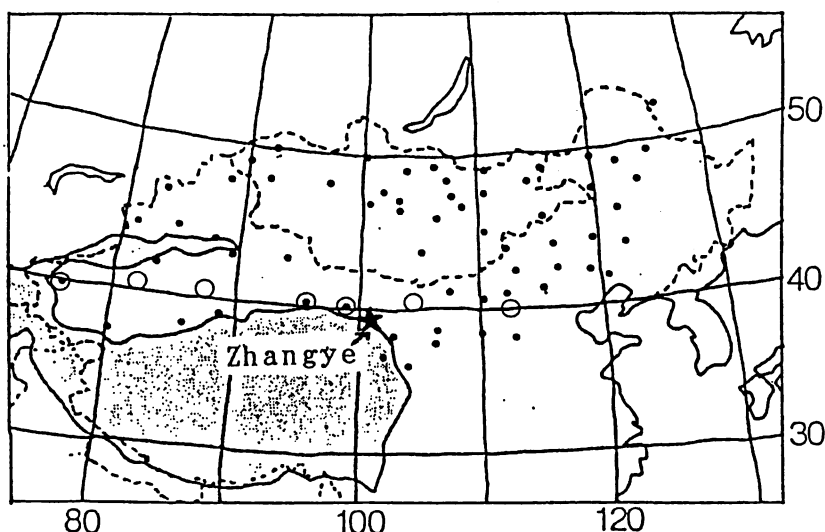


Fig.1. Geographical distribution of the observation stations. Black and white circles are the stations of monthly and daily precipitation used here. Zhangye (HEIFE station) is marked as the star.

daily precipitation records of China (several stations) in 1981 and 1982. The distribution of the stations of precipitation is shown in Figure 1. In order to calculate the water vapor transport, 3) the twice daily global data generated by the ECMWF (European Center For Medium Range Weather Forecast) global data assimilation systems were used from 1980 to 1989.

From the ECMWF data set we mainly utilize the 2.5x2.5 gridded data of wind and humidity for computing the amount of water vapor transport. Precipitable water, water vapor flux and its divergence are integrated in the whole troposphere and the lower layer of troposphere (from surface to 700hPa). We focus on the lower layer flux of the water vapor is used, since its convergence contributes most to precipitation.

The vertically integrated horizontal flux vector of water vapor was calculated by the following formula;

$$\bar{Q} = \int_{p_s}^{p_s} q \bar{V} \left(\frac{dp}{g} \right) \quad (1)$$

Neglecting condensed-phase water in the atmosphere, water balance equation can be written as ;

$$\frac{\partial W}{\partial t} + \nabla \cdot \bar{Q} = E - P \quad (2)$$

where E is the evaporation from the surface, P is the precipitation falling on the surface, ∇ is the horizontal divergence operator, p_s is the surface pressure, q is specific humidity, v is the horizontal wind velocity vector, and g is the gravity constant. The change of precipitable water ($\frac{\partial W}{\partial t}$) can be neglected when long term mean state (annual, seasonal) is considered. Then, divergence of Q represents the value of E-P.

3. Seasonal dependency of precipitation and its time and space structure of interannual variability.

Figure 2 shows the spatial pattern of mean annual total precipitation. Much precipitation occurs around Tianshan mountains. The contour lines seem to enclose the arid land, which shows less precipitation over Taklimakan desert. Figure 3 shows the ratio of a) summer (June to August) and b) spring (March to May) precipitation to the annual precipitation. Most part of this area have much rain in summer. Especially, to the north of Tibetan Plateau and in most part of Mongolia, summer precipitation occupies more than 70% of annual precipitation. The north of Tianshan mountain, the spring precipitation is comparable to the summer precipitation.

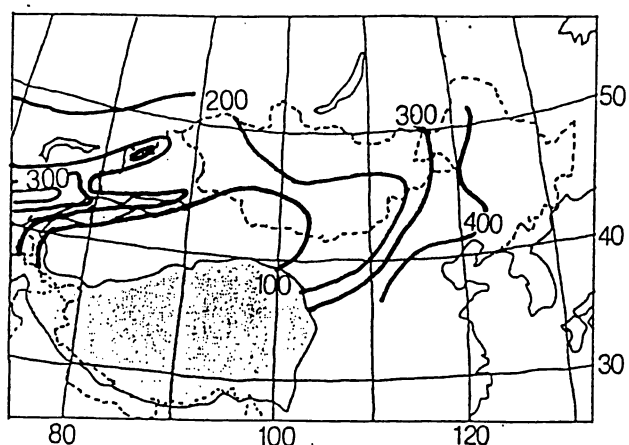


Fig.2. Mean annual precipitation. (mm)

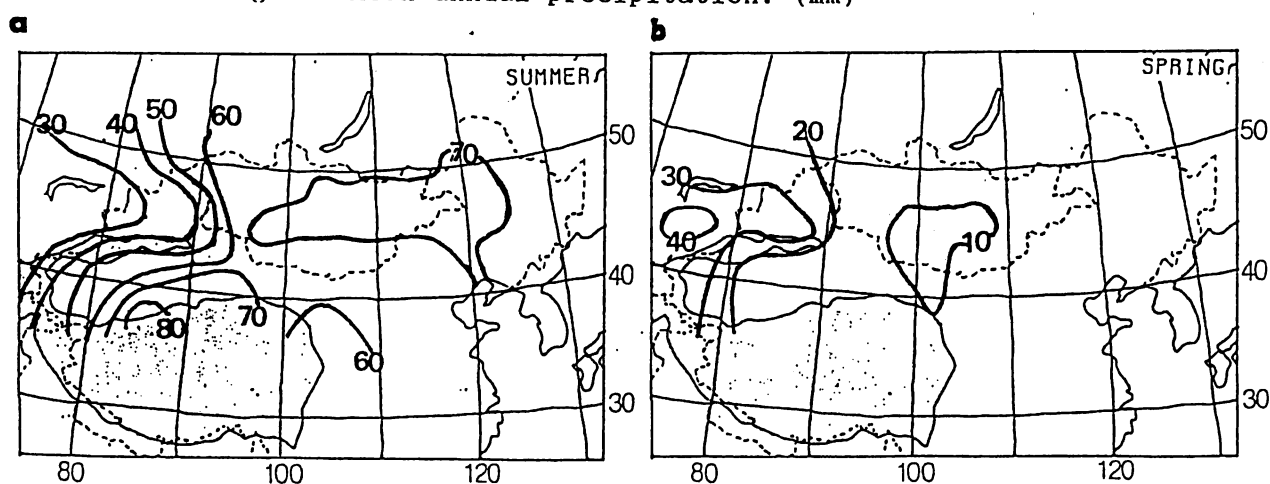


Fig.3. The ratio of the a) summer and b) spring precipitation to the annual precipitation. (Units are %)

Here we show the interannual variability of summer precipitation and its regionality, deduced from rotated EOF analysis. The summer precipitation data is the sum of monthly precipitation from June to August. We take cubic roots of original variables to make new variables which obey the Gaussian distribution. The first 6 EOFs are orthogonally rotated.

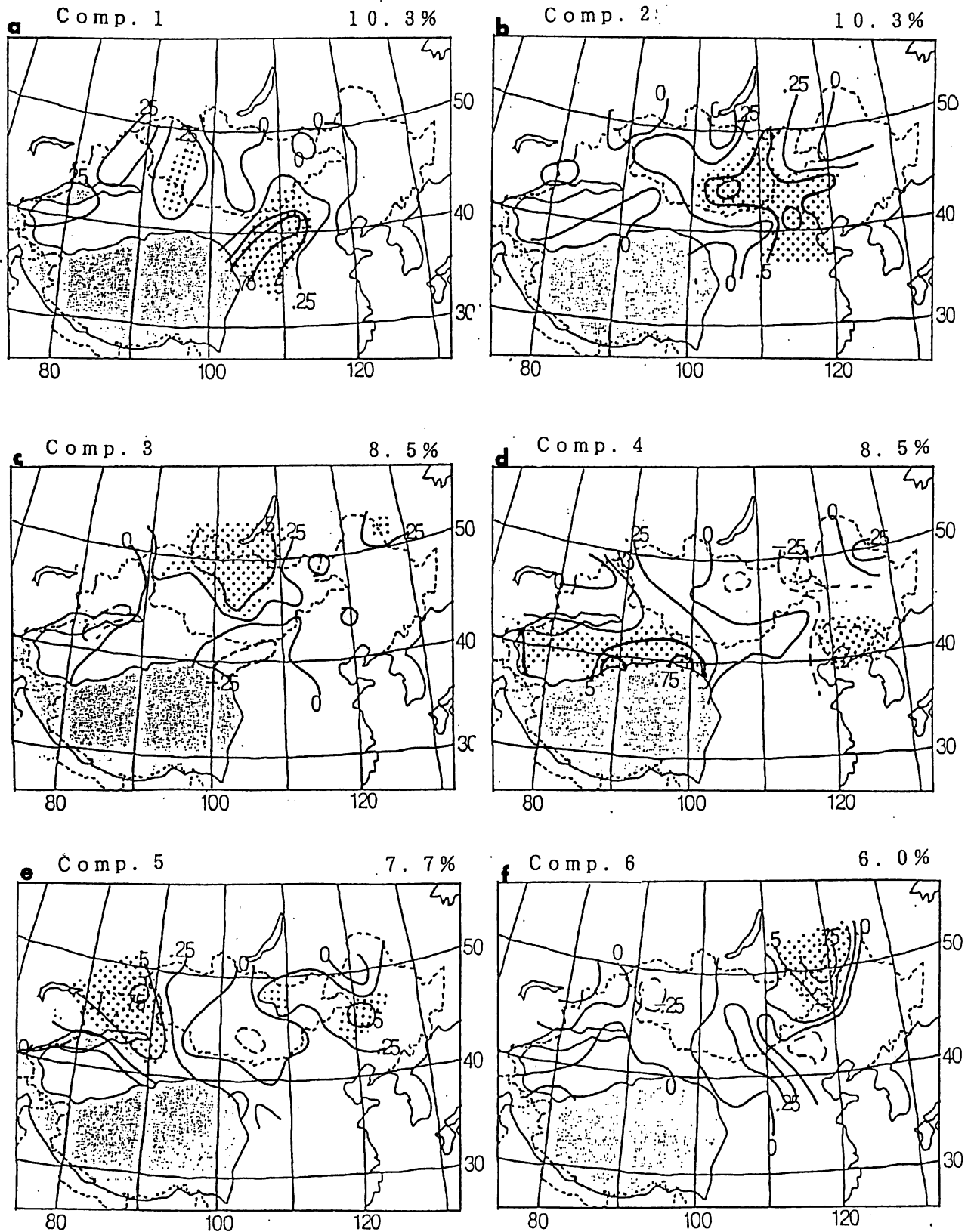


Fig.4. The factor loading values of the first six r-EOF components. Dots indicate regions of values exceeding .4(1% confidence level).

Figure 4 shows the factor loading patterns of the dominated components. The proportion of each components (after rotation) is shown in Fig. 4. Figure 5 shows the six areas determined basically by these components. The factor loading presents the correlation between each score time series and that of original data at the station. The dots indicate the area with statistically significant correlation beyond 1% confidence level(.40). The time series of these scores are shown in Figure 6(solid line). The dashed lines are standardized original precipitation fluctuation averaged in each area in Fig.5.

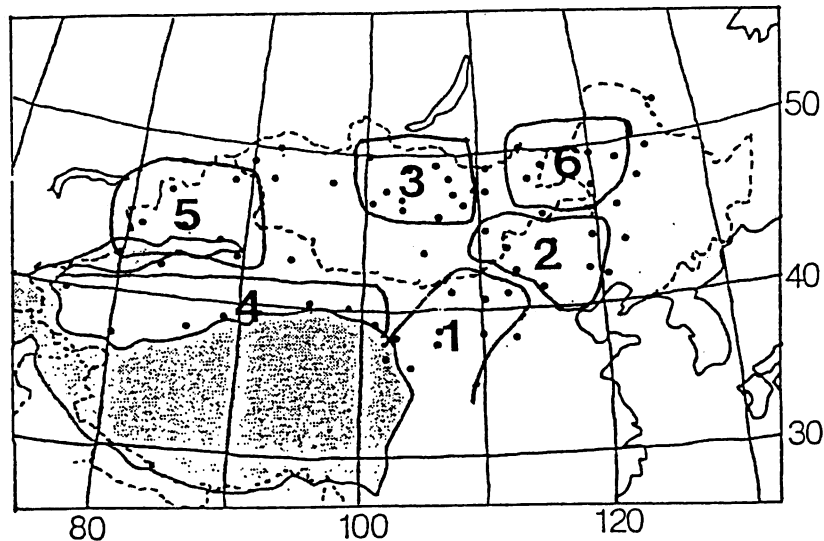


Fig.5. The 6 dominant areas deduced from rotated EOF. The mean original time series(dashed line in Fig.6) are calculated in these boxes.

HEIFE station of Zhangye, has the highest factor loading value in component 4. It is the east edge of that region and just east of the station the first component is dominated.

Here we describe the characteristics of each component.

The first component shows the variability around middle reach of Yellow River in Nei-Mongol, China. This area is nearly the same region where the precipitation are related to ENSO phenomena by Wang and Li(1990). Furthermore, this pattern is consistent with the northern part of the first EOF mode applied to whole China summer precipitation by Tian and Yasunari(1992) . They showed a see-saw between the Yellow River basin and the Yangtze River basin on the two to four year time-scales. The two to three year oscillation is seen in Fig.6a and this time series resemble to the first EOF score of Tian and Yasunari(1992). The western part of Mongolia seems to show the same phase with that region.

The second and third components show the variability in the North China (and eastern part of Mongolia) and the middle part of Mongolia, respectively. Time series of the second component and dominated areal mean

time series (solid and dashed line in Fig.6b) seems to have decreasing trend. In the time series of the third component decreasing trend is seen in 1960s and 1970s.

The fourth component shows the variability around Taklimakan desert, and Zhangye (HEIFE station) have statistically significant value in this component. Negative significant value is seen in the south part of North-east China. The time series also shows a decadal scale oscillation. The year to year amplitude is large in the last ten years.

The fifth and sixth components shows the variability of north of Tianshan mountains and the northernmost part of China, respectively.

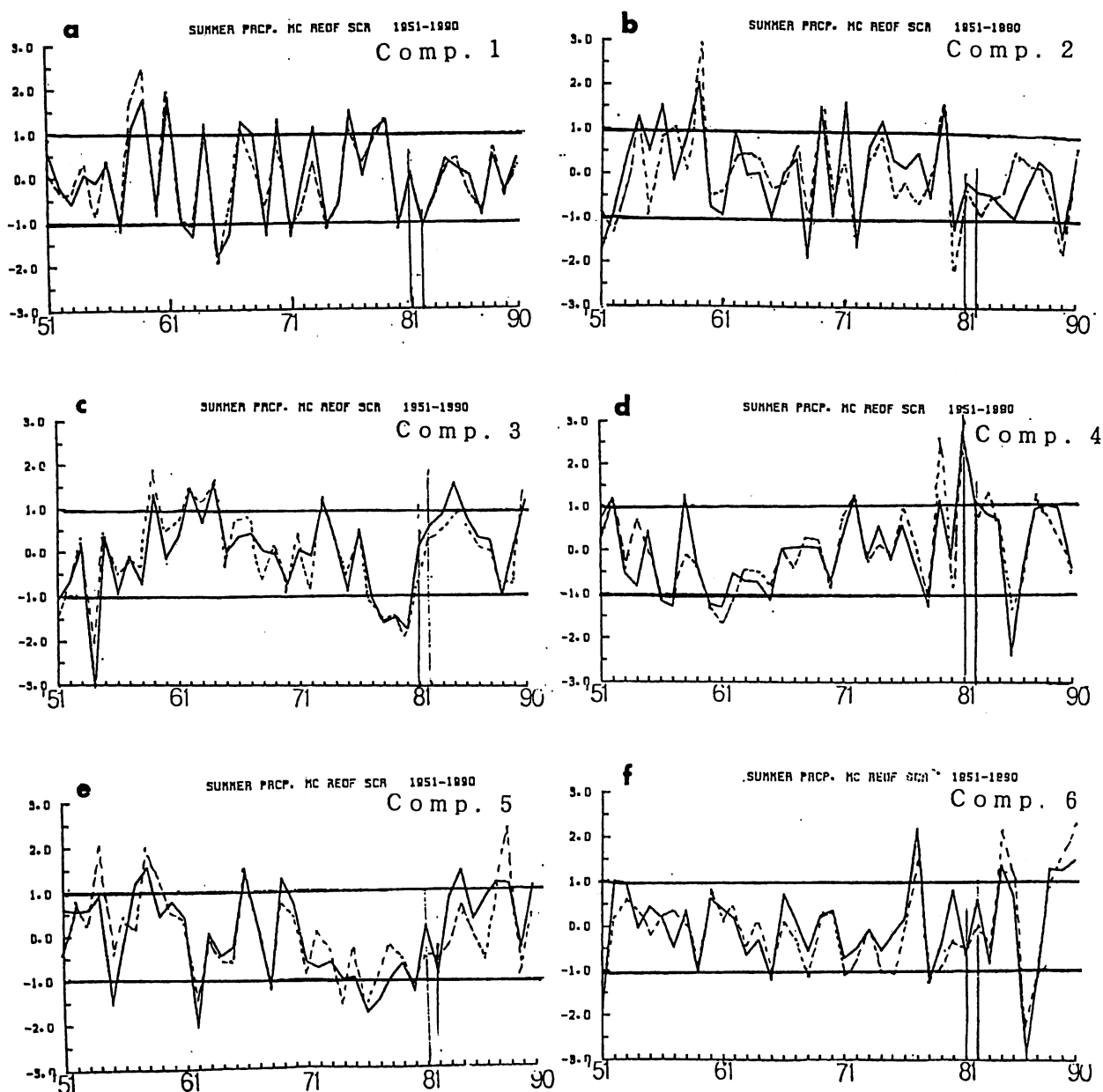


Fig.6 The scores of the rotated EOF analysis.

4. Mean water vapor transport in summer

Figure 7 shows the 10 year(1980-1989) mean summer water vapor transport integrated a) of total layer and b) from surface up to 700hPa. Two main courses of water vapor transport seem to flow to North and Northeast China and Mongolia; 1. westerly flow from India which turn northward over China, and 2. Northwesterly flow from Siberia. Taklimakan desert receives the water vapor transported from the west part of that region in Fig. 7 a), whereas in the lower layer, it comes turning along the Tianshan mountains from the northwest. The water vapor transport to the HEIFE observing station is not clear in these seasonal mean figure, so closer study with precipitation phenomena is necessary.

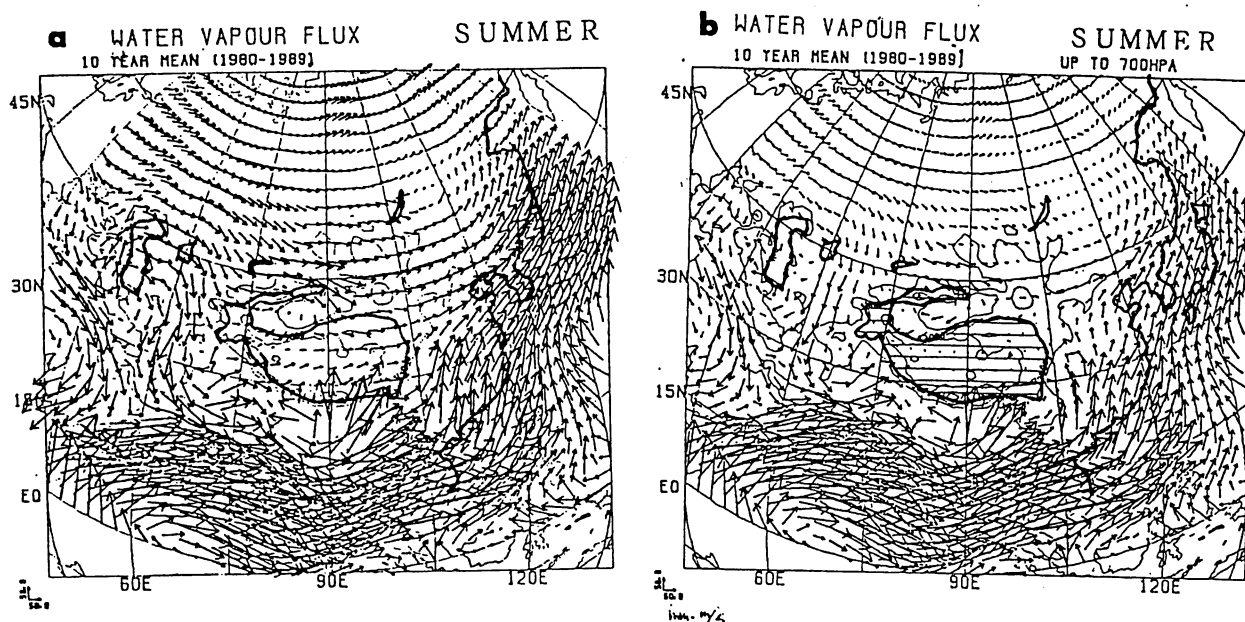


Fig.7 Ten year mean summer water vapor transport calculated in a) the whole troposphere and b) the lower troposphere(up to 700hPa).

4. Water vapor transport in 1981 and 1982, and case study

In order to examine the spatial pattern of water vapor transport more precisely, we choose contrastive two years; 1981 and 1982. In this study, the 4th component(Taklimakan desert, HEIFE station) has especially much precipitation in 1981 and relatively much in 1982(Fig.6d). While the 1st component(middle Yellow river basin) have normal precipitation in 1981, but less precipitation is noticeable in 1982(Fig.6a). The ENSO phenomena occurred in the year 1982, and some previous studies (e.g., Wang and Li(1990)) shows that in ENSO year the area around Gobi, arid and semi-arid region of the North part of China, receives less precipitation than normal year. Besides, the Indian monsoon was relatively normal in 1981, but weak in 1982.

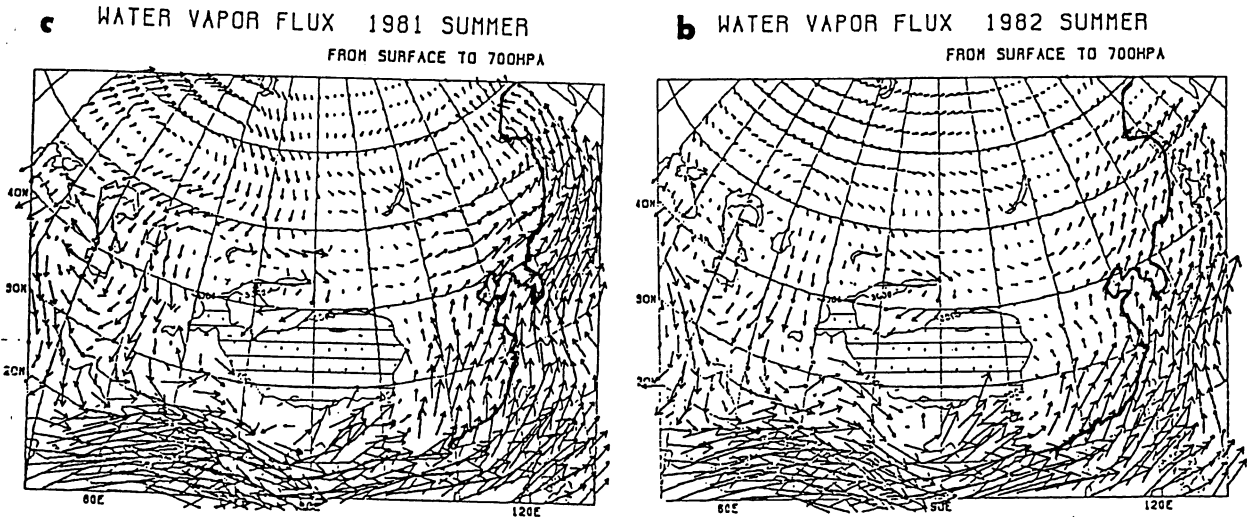
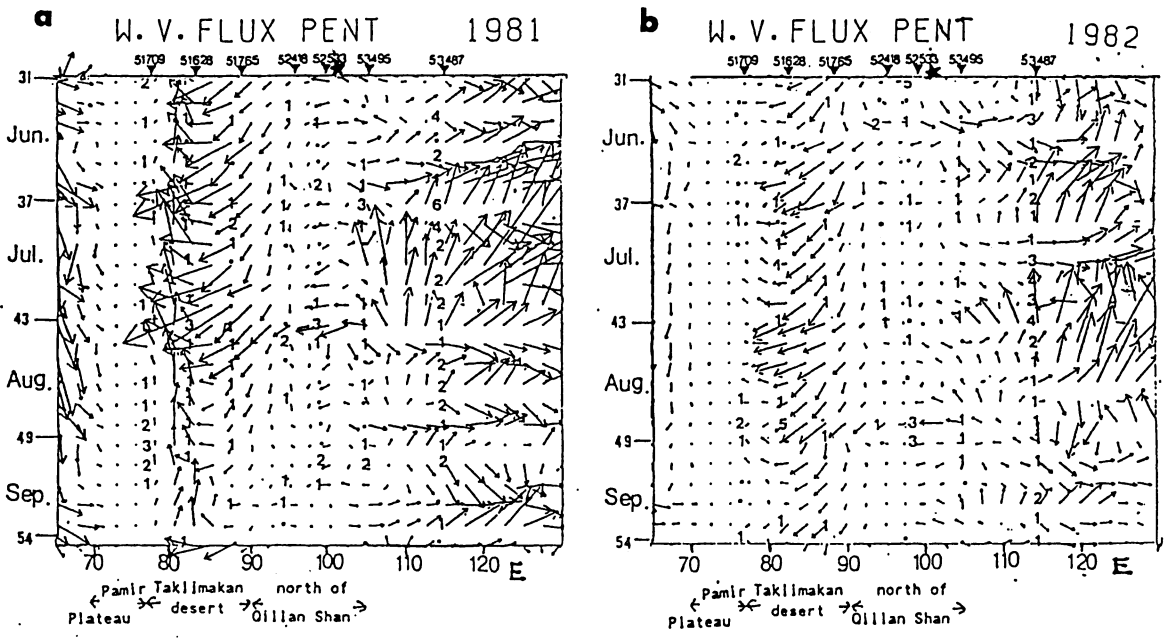


Fig.8 The water vapor transport of the lower troposphere in the summer of (a)1981 and (b) 1982.



Mark	Precipitation
.	$P \leq 1mm...$
1	$1 < P \leq 10$
2	$10 < P \leq 20$
3	$20 < P \leq 30$
4	$30 < P \leq 40$
5	$40 < P \leq 50$
6	$50 < P \leq 60$

Fig.9 The time-longitude cross section of water vapor flux and the concurrent precipitation index for 7 stations around 40°N. The stations are shown in Fig.1 with white circles.

Figure 8 shows the water vapor flux of the lower layer in summer of a)1981 and b)1982. A remarkable difference between the two years is perhaps due to found in this monsoon circulation. In 1982 the main flux of water vapor shifted eastward about 10 degrees in longitude. When we compare the flux flowing into Taklimakan between the two years, the flux is more disordered in 1981. In the continental-scale, the transport pattern in Central Asia and Far east Asia shows a remarkable meander in 1981.

To understand the difference of seasonal precipitation between the two years, pentad mean water vapor transport is examined. Figure 9 shows the time-longitude cross section of water vapor flux and the concurrent precipitation index for 7 stations around 40°N. The numbers in the section denote the magnitude of precipitation (see the caption of Fig.9). Over the Taklimakan desert (75°E - 90°E) a remarkable difference is seen between the two years. In 1981 larger vector i.e., water vapor transport from northeast in this season are larger than 1982.

To the north of Qillan Shan(90°E - 105°E), the precipitation is noticed when the vapor comes from the east in most cases. In 1982 less precipitation is noted in summer also to the north of Qillan Shan, and the difference of precipitation around there seems to be due to the changes in the monsoon circulation from the south. The eastward shift of water vapor transport of about 10° longitude is noticeable in 1982, as seen in Fig.8.

Figure 10a shows the two pentad mean spatial pattern of water vapor transport in the 43th pent in 1981, and Fig.10b shows that of 48th pent of 1982. In both cases, large water vapor comes from the south to Zhangye(HEIFE station) and the north of Qillan Shan mountain. This flow pattern is different from the mean state shown in Fig.8, but in most cases which precipitation occurred in north of Qillan Shan, the water vapor flux shows similar pattern compared to its periphery.

Many studies have pointed out the interannual variation of summer precipitation in China is mainly due to the change of the location of Pacific High Pressure. In the ENSO year, more precipitation occurs in summer around Chang Jiang river basin, while less summer precipitation is

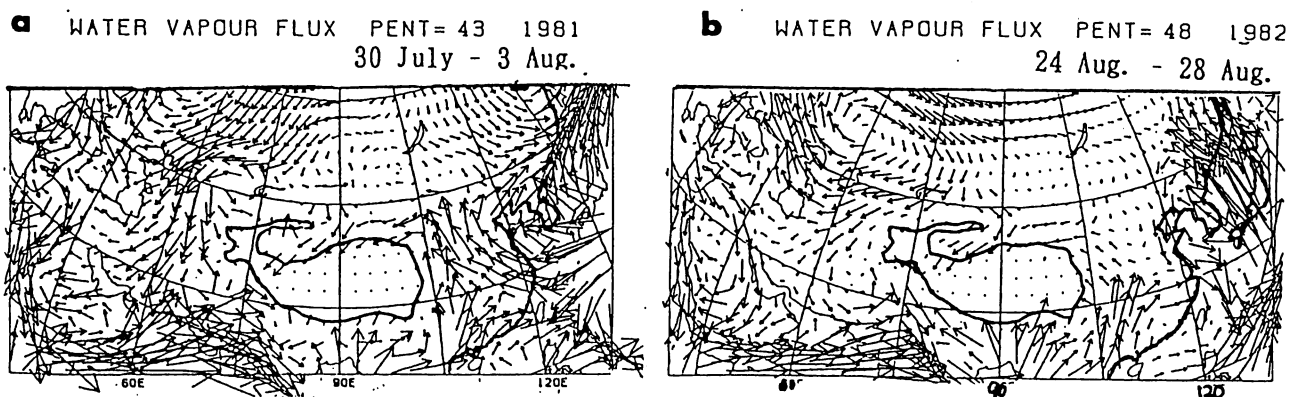


Fig.10 Pentad mean water vapor transport in a) 43th pent of 1981 and b) 48th pent of 1982.

seen around Huang He river basin. Huang and Wu(1989) presented that in the ENSO year, the northwestward extend of Pacific High is weakened and the lower reaches of Chang Jiang were not covered by the west edge of Pacific High, i.e. much rain are there. In the ENSO year of 1982, we found the same difference of Pacific High. In 1981, the western edge of the Pacific High extended northwestward and the main current of the water vapor transport came into the interior continent.

7. Conclusion

This study presented that the time-space structure of summer precipitation variability in the arid and semi-arid regions of China and Mongolia. The water vapor transport influences over these areas were compared between the two contrastive years, 1981 and 1982. The results are summarized as follows ;

(1) The summer precipitation accounts for 50% to the annual precipitation except for the north of Tianshan mountains. In the northwest of Tianshan mountains, spring precipitation is comparable with, or more, to that of summer.

(2) By applying rotated EOF analysis to the summer precipitation of arid and semi-arid regions of China and Mongolia, 6 regions are identified. Zhangye (HEIFE station) is located in one region covering Taklimakan desert.

(3) The northern part of China and Mongolia receive water vapor from the northwest, and Taklimakan desert receives water vapor transported along the periphery of Tianshan mountains from the northwest in the lower troposphere. Therefore the precipitation of the most part of Tarim basin is influenced mainly by the westerly circulation over Eurasia.

(4) Just north of Qilian Shan mountains (including HEIFE station), when large precipitation occurs, water vapor comes from the east. This water vapor seems to be transported from the south as part of the monsoon circulation over southeast Asia.

References

- Wang W.-C. and K.Li, Precipitation fluctuation over semi arid region in Northern China and the relationship with El Nino/Southern Oscillation. J. Climate, 3, 769-783, 1990.
- Huang, R.H. and Wu, Y.F., The influence of ENSO on the summer climate change in China and its mechanism. Adv. Atmos.Sci. Vol. 6, 21-30, 1989.
- Tian, S.F. and T. Yasunari, Time space structure of interannual variations in summer rainfall over China, J.Meteor.Soc. Japan, 70, 585-596, 1992.

Discussions

Q.(Kato): You have shown that the moisture flux toward the desert in China from the west mainly in the middle or upper troposphere, while the flux from the east is in the lower troposphere. This might suggest the difference of synoptic scale atmospheric systems contributing to the time mean water transport.

Do you have any idea about it ?

A. I don't have any idea now, but I will examine synoptic-scale atmospheric system as a next step.

Q.(Bolle): Did you compute the divergence / convergence of the water vapor flow and intercompare it with measured evaporation/precipitation data ?

A. No, I did not.

Q.(Singh): How do you demarcate the six regions that are non over lapping?

A. 0.4 loading contours on our EOF give these regions almost exclusively.